IM-OCDM for ISAC: Joint Communication and Sensing Using Index Modulation and LFM Radar

José Miracy de Souza Filho, George Lucas Lima Takemiya, and José Carlos Marinello Filho

***Abstract*— This work proposes an Index Modulation-based Orthogonal Chirp Division Multiplexing (IM-OCDM) waveform for integrated sensing and communication (ISAC) in future 6G systems. By embedding Linear Frequency Modulated (LFM) radar pulses into the inactive subchirps of a sparse IM-OCDM grid, the design enables joint radar-communication operation without spectral overhead. To accurately identify radar and communication subchirps, we propose deep learning classifiers operating on raw time-domain I/Q sequences. Two architectures are investigated: a CNN with gated recurrent units and attention (CNN-GRU-Att), and a CNN with Transformer-based attention including explicit SNR embedding (CNN-Transformer-Att). A large-scale dataset of 44,000 samples was generated across SNR levels (0–20 dB) and radar-to-communication power ratios from 0 to 3 dB—where radar signals are increasingly dominant. Results show that the Transformer-based model consistently outperforms the GRU-based counterpart in all regimes, reaching up to 96.3% F1-score and 99.3% Area Under ROC Curve (AUROC) under high SNR. Moreover, the Transformer exhibits improved robustness under noise and signal imbalance, confirming its suitability for dynamic ISAC environments. The proposed solution enhances spectral efficiency, sensing accuracy, and subchirp classification, providing a scalable physical-layer framework for next-generation ISAC systems**

***Keywords*— 6G, ISAC, IM-OCDM, radar, sensing, chirp signals, Transformers, GRU.**

I. Introduction

6G networks are envisioned to support seamless integration of communication and environmental sensing, enabling intelligent services such as autonomous driving, industrial automation, and immersive applications. Integrated sensing and communication (ISAC) is a foundational enabler for such applications, aiming to unify radar and communication operations within a common radio infrastructure [1], [2].

Conventional waveforms like orthogonal frequency division multiplexing (OFDM) exhibit high sidelobes, limited Doppler resilience, and poor autocorrelation, limiting their effectiveness in ISAC scenarios [3], [4]. Orthogonal chirp division multiplexing (OCDM) leverages chirp signals with inherent robustness against multipath fading and Doppler shifts [5]. However, Index Modulation (IM) in IM-OCDM enables sparse symbol transmission while leaving inactive subchirps underutilized [6].

José M. de Souza F., George L. L. Takemiya, and José C. Marinello F. are with the Department of Electrical Engineering, Federal University of Technology - PR, Cornélio Procópio - PR, e-mail: jmiracy@gmail.com, georgetakemiya@alunos.utfpr.edu.br, jcmarinello@utfpr.edu.br. This work was partially supported by CNPq through PIBIC under Grant No. 104331/2025-9, and by Araucária Foundation for Scientific and Technological Development Support of the State of Paraná (FA) under Grant PRD2023361000168.

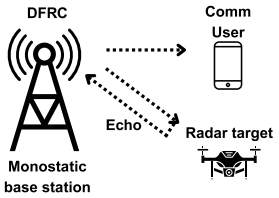

Fig. 1. Dual-Functional Radar Communications (DFRC) refers to joint systems that employ a shared, single transmitted waveform for both communication and radar functions. Monostatic defines the system for sensing topology (co-located TX).

This paper proposes an IM-OCDM framework that embeds LFM radar pulses [7] into inactive subchirps, enabling simultaneous radar and communication without additional bandwidth. Figure 1 illustrates the considered ISAC scenario.

Since the communication receiver cannot *a priori* determine which subchirps are allocated for communication, we introduce a **Convolutional Neural Network combined with a Transformer-based attention mechanism (CNN-Transformer-Att)**. This model captures both local spatial features and global dependencies within subchirp sequences, enabling accurate identification of communication subchirps.

Radar performance is benchmarked via the Cramér-Rao lower bound (CRLB), while communication efficacy is assessed using the data information rate (DIR). These metrics are jointly analyzed using a Tchebycheff scalarization method to evaluate trade-offs under varying signal-to-noise ratio (SNR) levels [8].

Main Contributions:

- An **IM-OCDM** waveform that embeds LFM radar pulses into inactive subchirps for ISAC operation, enhancing spectral efficiency without additional bandwidth requirements.
- A deep learning-based classifier framework using **CNN-GRU-Att** and **CNN-Transformer-Att** architectures, operating directly in time-domain received sequences for robust subchirp classification.
- A comprehensive performance evaluation incorporating **classification metrics** (Accuracy, Precision, Recall, F1, Area Under ROC Curve) and **ISAC metrics** (DIR, MI, CRLB).
- A **Tchebycheff-based multi-objective analysis** to assess the DIR–MI trade-off, revealing complementary strengths of GRU-based and Transformer-based classifiers under different SNR regimes.

The proposed IM-OCDM framework, together with deep learning-based classifiers, improves spectrum usage and sens-

ing accuracy, offering a scalable solution for real-time ISAC in future 6G systems.

A. Related Work

ISAC has emerged as a key enabler for 6G systems, motivating various waveform designs to jointly support communication and sensing. OFDM remains a baseline due to its maturity [9], but its high sidelobes and poor Doppler resilience limit performance in high-mobility scenarios [3]. Orthogonal time-frequency space (OTFS) improves robustness under mobility [5], though it incurs high equalization complexity. Chirp-based OCDM offers better Doppler and multipath resilience [5], yet previous approaches underutilize inactive subchirps.

The proposed IM-OCDM framework addresses this gap by embedding LFM radar pulses into inactive subchirps via index modulation, enhancing spectral efficiency without extra bandwidth. Furthermore, our CNN-Transformer-Att model with SNR embedding improves subchirp classification over traditional methods, supporting dynamic ISAC operation with scalability for 6G deployments.

II. System Model

The proposed IM-OCDM ISAC framework transmits communication and radar signals over orthogonal subchirps within the Fresnel domain. Communication subchirps are exclusively used for data transmission, while inactive subchirps are allocated for radar operations using LFM pulses. There is no physical overlap between radar and communication signals at the subchirp level.

The signal classification problem does not aim to separate physically superimposed signals within the same subchirp, but rather to distinguish which subchirps were allocated for communication *versus* radar within each IM-OCDM block. This corresponds to a binary classification task:

- Label **1**: subchirps used for communication (**COMM**).
- Label **0**: subchirps available for radar (**RADAR**).

This distinction is essential for ISAC scenarios where reliable identification of communication *versus* radar resources is required under channel impairments and noise. Figure 2 illustrates the general system architecture, highlighting this functional partitioning.

At the communication receiver, a CNN-Transformer network with attention distinguishes radar from communication content by learning spatio-temporal patterns in the time-domain received sequences, enabling robust classification across varying SNRs.

The architecture is benchmarked against an OFDM-based ISAC method [9] using identical simulation parameters. Key performance indicators include DIR for communication and MI for radar, adapted to the chirp-based structure.

A. Subchirp Signal Definition and Transmission

Each OCDM subchirp is represented in the Fresnel domain by an orthogonal linear chirp basis function. The basis function $\psi_k[n]$ is defined as:

$$\psi_k[n] = \frac{1}{\sqrt{N}} e^{j\pi\alpha(n-k)^2}, \quad 0 \leq n < N. \tag{1}$$

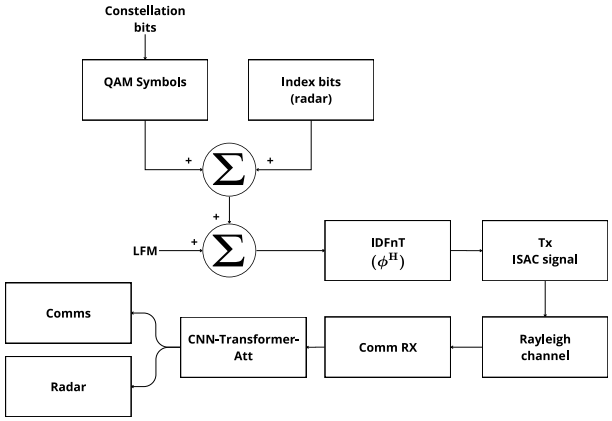

Fig. 2. General System Diagram.

The parameter α controls the chirp rate, and is calculated as $\alpha = B/N$, where B is the total bandwidth and N is the total number of subchirps.

The composite Fresnel-domain signal $\mathbf{X}$ is constructed by combining both communication and radar components:

$$\mathbf{X} = \mathbf{X}_{\text{comm}} + \mathbf{X}_{\text{radar}}, \tag{2}$$

where:

- $\mathbf{X}_{\text{comm}}$ contains k active subchirps modulated via IM with QAM symbols placed at indices of active communication subchirps Ω_{comm}.
- $\mathbf{X}_{\text{radar}}$ contains LFM radar pulses placed at indices $\Omega_{\text{radar}} = \{0, 1, ..., N-1\} \setminus \Omega_{\text{comm}}$.

The time-domain ISAC signal $x[n]$ is generated by applying the inverse Discrete Fresnel Transform (IDFnT) [7] to the composite Fresnel-domain signal:

$$x[n] = \text{IDFnT}\left(\mathbf{X}\right), \quad n = 0, 1, ..., N-1. \tag{3}$$

This time-domain signal $x[n]$ encapsulates both radar and communication functionalities in a single waveform, transmitted over the shared spectrum.

B. IM-OCDM ISAC Signal Generation and CNN-Transformer-Att Receiver

To ensure reproducibility, Table I summarizes the key characteristics of the generated dataset.

Signal Generation: The total N subchirps are divided into g subblocks, each with $n_c = N/g$ subchirps. In each subblock, k subchirps are activated for communication using index modulation combined with QAM (modulation order M), while the remaining $(n_c - k)$ subchirps are allocated for radar via LFM pulses. The composite signal is constructed in the Fresnel domain and converted to the time domain via IDFnT with a sampling rate F_s. The signal generation process is detailed in Algorithm 1.

Receiver: Two neural architectures are proposed for subchirp-level classification: (i) CNN-GRU-Att, which combines convolutional layers with Gated Recurrent Units (GRUs) to model temporal dependencies; and (ii) CNN-Transformer-Att, which replaces GRUs with a Transformer encoder to capture long-range dependencies via self-attention. Both models process time-domain received sequences and incorporate a

TABLE I
DATASET AND CNN+TRANSFORMER+ATT SETUP FOR IM-OCDM ISAC

Parameter	Value
Dataset	
Total Samples	44,000
SNR Range (dB)	0–20 in steps of 2
Power Ratio (dB)	0–3 in steps of 1
Subchirps per Sample (N)	256
Subblocks per Frame (g)	8
Comm/Radar Split	$\sim$58% / 42%
Channel Model	Rayleigh fading + AWGN
Modulation	16QAM
Bandwidth	1 MHz
Subchirp Activation	Weighted random: $1 + 2 \cdot \text{rand}(1, n_c)$
Model Hyperparameters	
CNN Filters	[32, 64]
Transformer Layers	3
Attention Heads	8
Embedding Dim. (d)	64
SNR Embedding	64-D MLP
Optimizer / LR	Adam / 10^{-3}
Batch Size / Epochs	32 / 300
Loss / Criterion	BCE / Max F1-score

normalized SNR parameter as an additional input. The SNR is transformed into an embedding vector $\mathbf{u} \in \mathbb{R}^{N \times d_u}$, which is concatenated with features extracted by a shared CNN-based feature extractor. The combined features $\mathbf{Z}$ are then added to a trainable positional encoding (PosEnc)[1] before being processed by an attention pooling layer for final classification. The inference pipeline, including SNR embedding, is detailed in Algorithm 2 for both classifiers. Their performance is compared in Section III.

Algorithm 1 IM-OCDM ISAC Signal Generation

Require: N, g, k, M, F_s
Ensure: Time-domain ISAC signal $x[n]$
1: $n_c \leftarrow N/g$
2: Generate bitstream $\mathbf{b}$ of length $g \cdot \log_2 \binom{n_c}{k} + gk \log_2 M$
3: Split $\mathbf{b}$ into $\mathbf{b}_{\text{idx}}$ (index bits) and $\mathbf{b}_{\text{mod}}$ (modulation bits)
4: Map $\mathbf{b}_{\text{idx}} \rightarrow \Omega_{\text{comm}}$
5: QAM map $\mathbf{b}_{\text{mod}} \rightarrow \mathbf{s}$
6: Populate $\mathbf{s}$ into $\Omega_{\text{comm}} \rightarrow \mathbf{X}_{\text{comm}}$
7: Set $\Omega_{\text{radar}} = \{0, ..., N-1\} \setminus \Omega_{\text{comm}}$
8: Populate LFM into $\Omega_{\text{radar}} \rightarrow \mathbf{X}_{\text{radar}}$
9: $\mathbf{X} = \mathbf{X}_{\text{comm}} + \mathbf{X}_{\text{radar}}$
10: Apply IDFnT: $x[n] = \text{IDFnT}(\mathbf{X})$

C. Channel and Received Signal Model

The received signal is modeled under a frequency-flat Rayleigh fading channel with additive white Gaussian noise (AWGN) as:

$$y[n] = h \cdot x[n] + w[n], \tag{4}$$

where h is the complex fading coefficient (constant over the block) and $w[n]$ is zero-mean complex Gaussian noise.

The time-domain ISAC signal $x[n]$ is generated via the IDFnT: $\mathbf{x} = \mathbf{F}^H \cdot \mathbf{X}$, where $\mathbf{X}$ is the composite Fresnel-domain signal combining communication and radar components, and $\mathbf{F}^H$ is the IDFnT matrix (unitary matrix).

[1]PosEnc is a trainable vector of dimension $(N \times (d + d_u))$, added to the concatenated features to inject positional information before the Transformer.

Algorithm 2 ISAC Rx with CNN-Transformer/GRU-Att

Require: Time-domain signal $\mathbf{y}[n] \in \mathbb{C}^N$, normalized SNR scalar
Ensure: Subchirp classification labels $\hat{y}$
1: Separate Real and Imag: $\mathbf{y}[n] \rightarrow \mathbf{Y} \in \mathbb{R}^{N \times 2}$
2: Compute SNR embedding: $\mathbf{u} \in \mathbb{R}^{N \times d_u}$
3: Apply 1D CNN on $\mathbf{Y}$: $\mathbf{Z}_{\text{cnn}} \in \mathbb{R}^{N \times d}$
4: Concatenate features: $\mathbf{Z} = [\mathbf{Z}_{\text{cnn}} \,|\, \mathbf{u}] \in \mathbb{R}^{N \times (d + d_u)}$
5: Add positional encoding (PosEnc): $\mathbf{Z} \leftarrow \mathbf{Z} + \text{PosEnc}$
6: Feed $\mathbf{Z}$ to Transformer encoder (multi-head attention)
7: Apply sigmoid classifier: $\hat{y} \in [0, 1]^N$ (binary decision per subchirp)

At the receiver, the signal $\mathbf{y}$ is directly input to a **CNN-Transformer-Att** model. The CNN extracts local spatial features, while the Transformer encoder captures global dependencies through self-attention. Attention weights α_t are computed as:

$$\alpha_t = \text{softmax}\left(\mathbf{q}^\top \cdot \tanh(\mathbf{W}\mathbf{h}_t + \mathbf{b})\right), \tag{5}$$

where $\mathbf{h}_t \in \mathbb{R}^d$ is the hidden state at time t, $\mathbf{W} \in \mathbb{R}^{d \times d}$ is the weight matrix, $\mathbf{b} \in \mathbb{R}^d$ is the bias vector, and $\mathbf{q} \in \mathbb{R}^d$ is the learnable query vector in the attention mechanism. d denotes the latent feature dimension of the GRU or Transformer layers, a context vector $\mathbf{c}$ summarizes the sequence:

$$\mathbf{c} = \sum_{t=1}^{T} \alpha_t \mathbf{h}_t, \tag{6}$$

which feeds dense layers for final subchirp classification. This learning-based approach leverages the chirp-orthogonal signal structure and attention-driven feature selection for robust subchirp classification in noisy channels. T denotes the number of time samples per OCDM block, corresponding to the temporal length of the input sequence (*e.g.*, $T = 256$).

D. Performance Metrics

In Section III, we evaluate performance in terms of four metrics: DIR, MI, CRLB, and Tchebycheff scalarization.

1) Data Information Rate (DIR): The DIR represents the achievable communication rate considering both symbol modulation and index modulation. For IM-OCDM, it is:

$$\text{DIR}_{\text{total}} = \sum_{k \in \Omega_{\text{comm}}} \log_2\left(1 + |H_k|^2 \cdot \gamma\right) + \left\lfloor \log_2 \binom{n_c}{k} \right\rfloor, \tag{7}$$

where Ω_{comm} denotes the set of subchirp indices assigned for communication, $|H_k|^2$ is the channel power gain on subchirp k, $\gamma = \sigma_x^2/\sigma_n^2$ is the transmit SNR, with σ_x^2 being the average transmit power per subchirp, and σ_n^2 the noise power. The first term accounts for modulation capacity, while the second term captures the information conveyed by index modulation (IM) bits.

2) Mutual Information (MI): The MI metric evaluates sensing information content for radar subchirps, considering

the channel gain and power allocation. It is given by:

$$\text{MI} = \frac{1}{2} \sum_{k \in \Omega_{\text{radar}}} \log_2\Big(1 + |H_k^{(r)}|^2 \cdot \rho \cdot \gamma\Big), \tag{8}$$

where Ω_{radar} is the set of radar-allocated subchirps, $|H_k^{(r)}|^2$ is the radar channel gain, and $\rho = 10^{\text{PR}/10}$ is the power allocation ratio in linear scale, with PR ranging from 0 to 3 dB. The factor $\frac{1}{2}$ reflects the real-valued nature of radar information.

3) CRLB – Range Bound: The CRLB expresses the minimum achievable variance for unbiased estimators of time-delay (τ) and range (R) in radar sensing:

$$\text{CRLB}(\tau) = \frac{1}{8\pi^2\beta^2|H_k^{(r)}|^2\rho\,\gamma\,T_s}, \tag{9}$$

where $\beta = B/\sqrt{12}$ is the RMS bandwidth, and T_s is the symbol duration.

4) DIR–MI Trade-off:

$$\text{Tcheby} = \max\Big(\omega_1\big(\tfrac{\text{DIR}^* - \text{DIR}}{\text{DIR}^*} + \xi S\big),\ \omega_2\big(\tfrac{\text{MI}^* - \text{MI}}{\text{MI}^*} + \xi S\big)\Big), \tag{10}$$

where $S = \frac{\text{DIR}^* - \text{DIR}}{\text{DIR}^*} + \frac{\text{MI}^* - \text{MI}}{\text{MI}^*}$, DIR* and MI* are the utopia points (maximum achievable DIR and MI), ω_1 and ω_2 are weights satisfying $\omega_1 + \omega_2 = 1$, with ω_1 prioritizing DIR and ω_2 prioritizing MI, and $\xi = 0.01$ is an augmentation coefficient to avoid weak Pareto-optimal solutions. This scalarization approach traces the Pareto front for DIR–MI trade-offs.

E. Classification Performance Metrics

The following metrics are used to evaluate the classification performance of the proposed models:

- **Accuracy:** proportion of correctly classified subchirps over the total number of subchirps.
- **Precision:** ratio of true positives to predicted positives.
- **Recall:** ratio of true positives to actual positives (also known as sensitivity).
- **F1-score:** harmonic mean of precision and recall, representing balanced performance.
- **AUROC (Area Under ROC Curve):** overall ability to distinguish between radar and communication labels across thresholds.

All metrics are reported globally and segmented by SNR and power ratio (PR) levels to assess robustness under channel variation and signal dominance conditions.

F. Computational Complexity Considerations

The proposed models deliver robust classification and sensing performance, though computational complexity is key for real-time embedded deployment. Transmitter-side IDFnT processing scales at $\mathcal{O}(N \log N)$, akin to IFFT. Receiver-side CNN-GRU-Att incurs $\mathcal{O}(Td^2)$ complexity, limiting GPU parallelization due to its sequential nature. Conversely, CNN-Transformer-Att scales at $\mathcal{O}(T^2 d)$, leveraging parallelizable self-attention across subchirps for faster inference on optimized hardware. For embedded systems, model compression, hardware acceleration, or SNR-aware switching is recommended. Future work will profile inference time and resource usage under real-time constraints.

III. Results and Discussion

Table II presents the key simulation parameters adopted from [9] to obtain the numerical results presented in this section.

TABLE II
KEY SIMULATION PARAMETERS: OFDM-ISAC VS. IM-OCDM-ISAC

Parameter	OFDM	IM-OCDM
Modulation	16QAM	16QAM
Waveform	OFDM	OCDM + LFM
Resources	256 carriers	256 subchirps
Comm/Radar Split	128/128	∼58%/42%
Samples	–	44k
SNR (dB)	0–20	0–20
Power Ratio (dB)	–	0,1,2,3
Signal Format	I/Q	I/Q
Sample Rate (MHz)	2	2
Bandwidth (MHz)	1	1
Symbol Duration (μs)	64	64
Channel	Rayleigh + AWGN	
Target Parameters	3600 m, 40 m/s	

A. Comparative ISAC Performance Analysis and Design Insights

Fig. 3 illustrates the ISAC performance of IM-OCDM at a PR of 3 dB and SNR ranging from 0 to 20 dB. DIR and MI grow with SNR, while CRLB decreases, confirming the inherent trade-off between communication and sensing. Subplot (d) shows the DIR–MI trade-off curve obtained using Tchebycheff scalarization. The point highlighted by a black star represents the configuration that *minimizes the Tchebycheff metric*, under PR = 3 dB, across all evaluated allocations and SNR values. This Tchebycheff-optimal point occurs at SNR = 20 dB, achieving DIR = 958.98 bits, MI = 709.86 bits (close to its utopia value), and CRLB = 142.57 m, with weights $\omega_1 = 0$ (full MI priority). This configuration minimizes the scalarization to 1.43×10^{-3}, demonstrating IM-OCDM's capability to prioritize radar observability while maintaining high communication performance.

TABLE III
COMPARISON BETWEEN IM-OCDM (TCHEBYCHEFF-OPTIMAL) AND REFERENCE [9] (RANDOM)

Configuration	DIR [bits]	MI [bits]	CRLB [m]
Reference (Random)	1,491.1	764.19	N/A
IM-OCDM (Tcheby-optimal)	958.98	709.86	142.57

Although this Tchebycheff-optimal point achieves lower DIR compared to the random configuration in [9], IM-OCDM reaches the MI upper bound while ensuring flexibility in resource allocation. Unlike OFDM-based baselines, IM-OCDM dynamically redistributes subchirps between radar and communication, enabling adaptive operation under heterogeneous ISAC requirements. This flexibility makes IM-OCDM particularly suitable for 6G scenarios, where on-demand sensing–communication trade-offs are critical.

B. Neural Network Performance Analysis

Tables IV and V show the classification results of CNN-Transformer-Att and CNN-GRU-Att (both with SNR embedding) under different SNR and PR conditions.

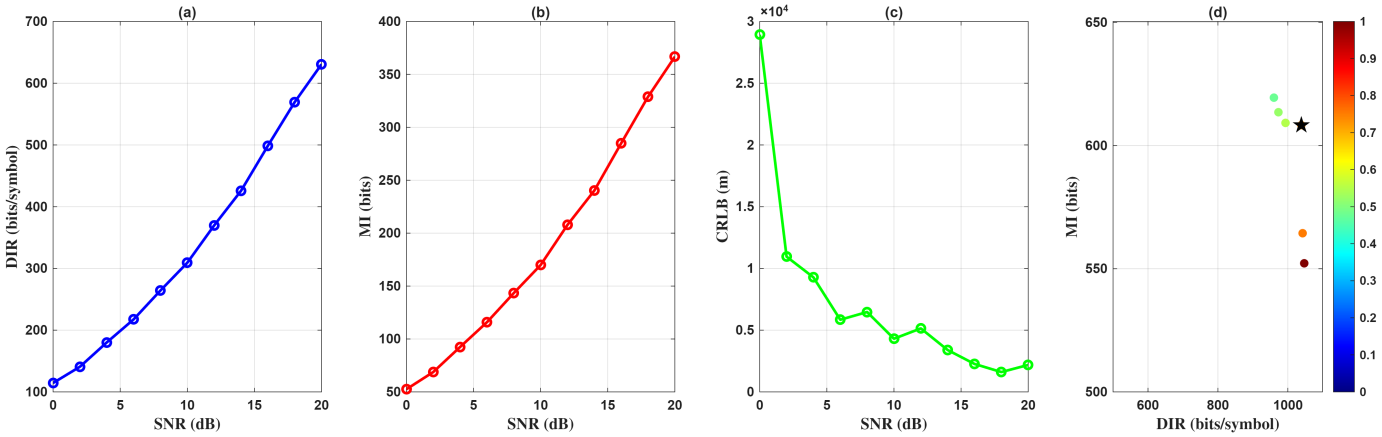

Fig. 3. ISAC performance metrics for PR = 3 dB: **(a)** DIR versus SNR, **(b)** MI versus SNR, **(c)** CRLB versus SNR, and **(d)** DIR–MI trade-off obtained using Tchebycheff scalarization. The color scale in (d) represents the weight ω_1 assigned to DIR in the scalarization function ($\omega_2 = 1 - \omega_1$). The black star marks the configuration that minimizes the Tchebycheff metric (Tchebycheff-optimal point).

The Transformer consistently outperforms the GRU across all metrics. At low SNR (0–6 dB), it achieves F1 = 0.791 vs. 0.711 for GRU; at medium SNR (7–13 dB), the gap widens (F1 = 0.904 vs. 0.754); and at high SNR (14–20 dB), Transformer approaches near-perfect accuracy (F1 = 0.944, AUROC = 0.983). For PR = 3 dB, Transformer reaches F1 = 1.000 and AUROC = 1.000, while GRU scores F1 = 0.963 and AUROC = 0.993. These results confirm that SNR embedding with self-attention enhances robustness for dynamic ISAC environments.

TABLE IV

PERFORMANCE VS. SNR (PR=3DB)

SNR	Model	F1	Acc.	Recall	AUROC
Low	TF+SNR	0.791	0.791	0.752	0.867
	GRU+SNR	0.711	0.694	0.714	0.767
Medium	TF+SNR	0.904	0.903	0.860	0.955
	GRU+SNR	0.754	0.747	0.733	0.824
High	TF+SNR	0.944	0.943	0.900	0.983
	GRU+SNR	0.769	0.763	0.747	0.840

TABLE V

PERFORMANCE VS. PR (SNR = 20DB)

PR	Model	F1	Acc.	Recall	AUROC
0 dB	TF+SNR	0.904	0.900	0.904	0.961
	GRU+SNR	0.823	0.816	0.817	0.898
3 dB	TF+SNR	1.000	1.000	1.000	1.000
	GRU+SNR	0.963	0.961	0.958	0.993

IV. CONCLUSION

This work proposed an IM-OCDM-based ISAC framework embedding LFM radar into inactive subchirps to enable dual functionality without extra spectrum. IM-OCDM surpassed OFDM in throughput and range precision while supporting flexible sensing–communication trade-offs. For reception, CNN-Transformer-Att with SNR embedding consistently outperformed the GRU baseline, achieving near-perfect performance at PR = 3 dB (F1 = 1.000, AUROC = 1.000). SNR embedding and attention mechanisms proved essential for robustness under dynamic conditions. Future work will target Doppler resilience, MIMO/multiuser extensions, and scalable Transformer designs. IM-OCDM combined with attention-based receivers shows strong potential for 6G ISAC deployments.

REFERENCES

[1] N. González-Prelcic, M. F. Keskin, O. Kaltiokallio, M. Valkama, D. Dardari, X. Shen, Y. Shen, M. Bayraktar, and H. Wymeersch, "The Integrated Sensing and Communication Revolution for 6G: Vision, Techniques, and Applications," *Proceedings of the IEEE*, pp. 1–0, 2024.

[2] W. Zhou, R. Zhang, G. Chen, and W. Wu, "Integrated Sensing and Communication Waveform Design: A Survey," *IEEE Open Journal of the Communications Society*, vol. 3, pp. 1930–1949, 2022.

[3] A. Chakravarthi Mahipathi, B. Pardhasaradhi, P. Lingadevaru, P. Srihari, J. D'Souza, and L. Reddy Cenkeramaddi, "A Survey on Waveform Design for Radar-Communication Convergence," *IEEE Access*, vol. 12, pp. 75 442–75 461, 2024.

[4] M. S. J. Solaija, S. E. Zegrar, and H. Arslan, "Orthogonal Frequency Division Multiplexing: The Way Forward for 6G Physical Layer Design?" *IEEE Vehicular Technology Magazine*, vol. 19, no. 1, pp. 45–54, 2024.

[5] L. Giroto de Oliveira, B. Nuss, M. B. Alabd, A. Diewald, M. Pauli, and T. Zwick, "Joint Radar-Communication Systems: Modulation Schemes and System Design," *IEEE Transactions on Microwave Theory and Techniques*, vol. 70, no. 3, pp. 1521–1551, 2022.

[6] J. Liu, P. Yang, T. Q. S. Quek, Y. Xiao, and W. Xiang, "Orthogonal Chirp Division Multiplexing With Index Modulation," *IEEE Transactions on Communications*, vol. 72, no. 8, pp. 4577–4590, 2024.

[7] X. Ouyang and J. Zhao, "Orthogonal chirp division multiplexing," *IEEE Transactions on Communications*, vol. 64, no. 9, pp. 3946–3957, 2016.

[8] P. Wang, D. Han, Y. Cao, W. Ni, and D. Niyato, "Multi-Objective Optimization-Based Waveform Design for Multi-User and Multi-Target MIMO-ISAC Systems," *IEEE Transactions on Wireless Communications*, p. 1–1, 2024. [Online]. Available: http://dx.doi.org/10.1109/TWC.2024.3428705

[9] B. Yang, S. Zhao, and M. Yi, "Subcarrier Multiplexing OFDM-based Radar Communication Integration," in *2021 13th International Conference on Wireless Communications and Signal Processing (WCSP)*, 2021, pp. 1–5.